Eur Biophys J (2006) 35: 469–476
DOI 10.1007/s00249-006-0054-x

ARTICLE

**Jong Seol Yuk · Duk-Geun Hong · Jae-Wan Jung
Se-Hui Jung · Hyun-Soo Kim · Jeong-A Han
Young-Myeong Kim · Kwon-Soo Ha**

Sensitivity enhancement of spectral surface plasmon resonance biosensors for the analysis of protein arrays

Received: 22 July 2005 / Revised: 22 February 2006 / Accepted: 14 March 2006 / Published online: 7 April 2006

Abstract A novel method for sensitivity enhancement of spectral surface plasmon resonance (SPR) biosensors was presented by reducing the refractive index of the sensing prism in the analysis of protein arrays. Sensitivity of spectral SPR biosensors with two different prisms (BK-7, fused silica) was analyzed by net shifts of resonance wavelength for specific interactions of GST–GTPase binding domain of p21-activated kinase-1 and anti-GST on a mixed thiol surface. Sensitivity was modulated by the refractive index of the sensing prism of the spectral SPR biosensors with the same incidence angle. The sensitivity of a spectral SPR biosensor with a fused silica prism was 1.6 times higher than that with a BK-7 prism at the same incidence angle of 46.2°. This result was interpreted by increment of the penetration depth correlated with evanescent field intensity at the metal/dielectric interface. Therefore, it is suggested that sensitivity enhancement is readily achieved by reducing the refractive index of the sensing prism of spectral SPR biosensors to be operated at long wavelength ranges for the analysis of protein arrays.

Keywords Surface plasmon resonance · Protein arrays · Sensitivity enhancement · Spectral SPR biosensor

J. S. Yuk · J.-W. Jung · S.-H. Jung · H.-S. Kim
J.-A Han · Y.-M. Kim · K.-S. Ha (✉)
Department of Molecular and Cellular Biochemistry
and Nano-Bio Sensor Research Center,
Kangwon National University School of Medicine,
Chunchon, Kangwon-Do 200-701, South Korea
E-mail: ksha@kangwon.ac.kr
Tel.: +82-33-2508833
Fax: +82-33-2507263

D.-G. Hong
Department of Physics, Kangwon National University,
Chunchon, Kangwon-Do 200-701, South Korea

Abbreviations AFM: Atomic force microscopy · MUA: 11-Mercaptoundecanoic acid · EDC: *N*-ethyl-*N*′-(dimethylaminopropyl)-carbodiimide · NHS: *N*-hydroxysuccinimide · GST: Glutathione S-transferase · GST–PBD: GST–GTPase binding domain of p21-activated kinase-1 · SPR: Surface plasmon resonance

Introduction

Recently, protein arrays have become a promising platform for the study of proteomes (Zhu et al. 2001; Yuk and Ha 2005). Protein arrays that consist of several tens to thousands of different proteins immobilized on a solid surface such as metal, glass, and plastics have played an important role in proteomics, drug screening, medical diagnostics, food safety, and environmental testing, because they enable high-throughput analysis with low sample-volume format and low cost (Kodadek 2001; Haab et al. 2001.

Several techniques, based on protein labeling, such as sandwich immunoassay, enzyme-linked immunosorbent assay, and radioactive isotopic labeling have been reported for the analysis of protein arrays. In addition, nonlabeling methods as a direct detection technique have also been used for the analysis of protein arrays, such as surface-enhanced laser desorption/ionization mass spectrometry, atomic force microscopy (AFM), and surface plasmon resonance (SPR) (Zhu and Snyder 2003; Wilson and Nock 2001; Li et al. 2004). Even though labeling methods as an indirect detection technique have good sensitivity performance compared to other nonlabeling methods, there are some problems such as heterogeneity of fluorescence labeling of proteins, the requirement for two specific binding reagents, and perturbation of protein activity caused by labeling. SPR has been used as a powerful technique among the analysis techniques of protein arrays because SPR allows real-time monitoring of biomolecular interactions

without labeling molecules. However, SPR-based biosensors have the problem of low sensitivity, compared to the labeling techniques in the analysis of protein arrays. For the purpose of sensitivity enhancement of SPR biosensors, several approaches as biochemical and physical methods have been reported, such as using colloidal Au (Lyon et al. 1998), dye (Hanning et al. 1999), liposome (Wink et al. 1998), latex particles (Kubitschko et al. 1997), hydrogel nanospheres (Okumura et al. 2005), surface plasmon active metal (Homola 1997), and incidence angle (Akimoto et al. 2000; Yuk et al. 2005). However, there have been no reports on the sensitivity enhancement of spectral SPR biosensors just by using the sensing prism without changing the incidence angle, surface plasmon active metal, or the additional nanomaterials for the analysis of protein arrays.

In this paper, we report on the sensitivity enhancement of spectral SPR biosensors by using the refractive index of the sensing prism for the analysis of protein arrays. The protein arrays were prepared by successively modifying with mixed thiols of 11-mercaptoundecanoic acid (MUA) and mercaptohexanol, GST–GTPase binding domain of p21-activated kinase-1 (PAK1) (GST–PBD), and anti-GST. The surface morphology of gold and mixed thiols was analyzed by AFM. Spectral SPR biosensors with low refractive index of the prism showed higher sensitivity than those with high refractive index of the prism at the same incidence angle, and this was discussed by the penetration depth of the evanescent field wave at the metal/dielectric interface.

Materials and methods

Chemicals and reagents

Octadecylmercaptan, octadecyltrichlorosilane, mercaptohexanol, MUA, tetracarbone chloride, cyclohexane, and ethanolamine were obtained from Sigma (St. Louis, MO). *N*-hydroxysuccinimide (NHS) and *N*-ethyl-*N*′-(dimethylaminopropyl)-carbodiimide (EDC) were from Pierce (Rockford, IL). Monoclonal anti-RhoA and anti-rac1 were purchased from Santa Cruz Biotechnology (Santa Cruz, CA). GST–PBD was purified by expressing the genes in *Escherichia coli* (BL21) and purified according to the procedures of a previous report (Leem et al. 1997). All other chemical reagents were of analytical grade.

Preparation and hydrophobic modification of gold arrays

Gold arrays with 50 spots (diameter of each spot, 2 mm) were fabricated by depositing Ti and Au (50 and 450 Å) films on slide glasses by using an RF-magnetron sputtering apparatus at a vacuum of 3×10^{-6} Torr. The gold arrays were cleaned by incubation with a cleaning solution of NH_4OH:H_2O_2:H_2O (1:1:5, v/v) at 70°C for 10 min and washed with distilled H_2O.

Hydrophobic modification of the glass surfaces of gold arrays was performed by successive incubation with octadecylmercaptan and octadecyltrichlorosilane to prevent protein solutions between spots from being mixed during protein incubation. Initially, the gold surfaces were coated with a monolayer of octadecylmercaptan by incubation with 5 mM octadecylmercaptan in ethanol for 16 h at room temperature and washed with ethanol. The arrays were then incubated with a mixture of cyclohexane/tetracarbone chloride/octadecyltrichlorosilane (20:5:0.04, v/v) to generate hydrophobic glass surfaces. After 30 min, they were washed with a mixture of cyclohexane/tetracarbone chloride (20:5, v/v) at 45°C, tetracarbone chloride at 45°C, and ethanol at room temperature, in this order. Finally, the octadecylmercaptan layer on the Au surfaces was removed by incubation with the cleaning solution at 70°C for 10 min to produce hydrophilic gold surfaces surrounded by hydrophobic glass surfaces.

Preparation of protein arrays

A schematic diagram of the protein array coupled with a prism is shown in Fig. 1. Gold surfaces were modified with a mixture of 1 mM MUA and 1 mM mercaptohexanol in ethanol for 16 h for the preparation of a self-assembled monolayer. For amine coupling between the carboxyl group of MUA and the amine group of proteins, the carboxyl group of MUA was activated by treating the thiol-modified gold surfaces with a solution of 50 mM NHS and 200 mM EDC for 10 min.

For the analysis of antigen–antibody interactions, 100 μg/ml of GST–PBD in 10 mM sodium acetate buffer (pH 4.5) was applied by a micropipette to the activated thiol surfaces of gold array spots at 37°C for 10 min. After incubation, the surfaces were washed

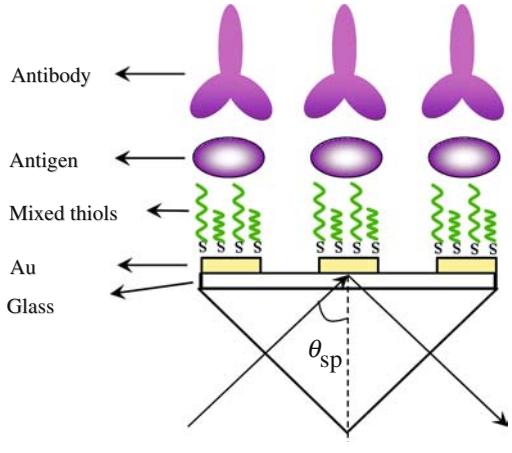

Fig. 1 Surface structure of protein arrays for spectral SPR biosensors. Proteins are immobilized on a linker layer which was formed by MUA and mercaptohexanol on the gold surface

twice with 0.1% Tween 20 in phosphate buffered saline (8.1 mM Na_2HPO_4, 1.2 mM KH_2PO_4, 138 mM NaCl, 2.7 mM KCl, pH 7.4) for 5 min, and rinsed with dH_2O. The residual carboxyl groups of MUA were deactivated by incubation with 1 M ethanolamine solution (pH 8.5) for 10 min. Then, the protein array was incubated with 10 mg/ml of bovine serum albumin in phosphate buffered saline (8.1 mM Na_2HPO_4, 1.2 mM KH_2PO_4, 138 mM NaCl, 2.7 mM KCl, pH 7.4) at 37°C for 10 min to reduce nonspecific interactions. The antigen–antibody interactions were investigated by introducing antibody GST to the immobilized GST–PBD on the mixed thiol surface. The antibody solutions (100 μg/ml) were prepared in a phosphate buffer (8.1 mM Na_2HPO_4, 1.2 mM KH_2PO_4, pH 7.4) and 2 μl of the antibody solution was applied to the antigen protein array at 37°C for 10 min. After incubation, the surfaces were washed twice with 0.1% Tween 20 in phosphate buffered saline (8.1 mM Na_2HPO_4, 1.2 mM KH_2PO_4, 138 mM NaCl, 2.7 mM KCl, pH 7.4) for 5 min, rinsed with dH_2O, dried under N_2 gas, and immediately analyzed by a spectral SPR sensor.

Atomic force microscopy

The surface roughness of gold and mixed thiols was measured by using AFM. AFM imaging was performed in air by using a Nanoscope IIIa (Digital Instruments, USA) in the contact mode and under the tapping mode. Nanoprobe cantilevers (spring constants of 0.12 and 0.38 N/m) with oxide-sharpened Si_3N_4 integral tips were used for the contact mode, and tapping silicon cantilevers with resonance frequencies of 280–320 kHz were used for the tapping mode. The applied force was varied from several nN to tens of nN in the contact mode. The film roughness was measured from images obtained by using the less destructive tapping mode, and the formation of a mixed thiol layer was investigated by the images with traces of an artificial hole that was made by scratching the layer surface by the contact mode.

Self-assembled spectral SPR biosensor

A wavelength interrogation-based SPR biosensor was self-constructed with the Kretschmann–Raether geometry of the attenuated total reflection (ATR) method. For the construction of the SPR biosensor, a quartz tungsten halogen lamp of 20 W (Oriel, Inc., USA) was used as light source because of its stable output. A polarizer was positioned in the input light path to obtain transverse magnetic polarized light. The incidence angle was adjusted to 46.2° by beam steering devices to obtain the resonance wavelength. The prism (1.517 at 589 nm for BK7, 1.458 at 589 nm for fused silica; Oriel, Inc., USA) combined with protein arrays by index-matching fluid was mounted on a motorized x–y linear stage (Cheung Won Mechatronics Co., Korea) controlled automatically by personal computer control. The reflected light from the protein arrays was collected into an optical fiber and then analyzed by an AVS-S2000 spectrometer (Avantes, Netherlands). The resolution of the AVS-S2000 spectrometer was 0.5 nm in the range of 500–770 nm. In order to collimate nonsymmetrical beams, plano-cylindrical glass lenses were positioned in front of the optical fiber. Motion control, data acquisition, analysis, and display were performed by self-developed programs based on the LabVIEW software.

Theory

Changes of the optical constants on the metal surface have a great influence on the resonance condition, which is the basis of SPR biosensors for biosensing purposes (Liedberg et al. 1983). SPR is an electromagnetic phenomenon in which an evanescent wave excites a charge density oscillation along a metal/dielectric interface. Surface plasmons are longitudinal or transverse magnetic charge density waves propagating along the metal/dielectric interface, and the electromagnetic surface waves, which have their maximal intensity on the metal surface, are exponentially decaying fields perpendicular to the surface (Raether 1988).

In the case of a metal film of finite thickness, the wave vector of surface plasmons is expressed as (Raether 1988; Pockrand 1978; Knobloch et al. 1996)

$$k_{sp} = k_{sp}^{(0)} + \Delta k_{sp}^{(1)}, \tag{1}$$

where $k_{sp}^{(0)} = (2\pi/\lambda)\{\varepsilon_m(\lambda)\varepsilon_d/[\varepsilon_m(\lambda) + \varepsilon_d]\}^{1/2}$ for a plate surface of a semi-infinite metal with the complex dielectric function $\varepsilon_m(\lambda) = \varepsilon_{mr} + i\varepsilon_{mi}$, λ is the free-space wavelength of light and ε_d is the dielectric constant of the dielectric on metal. SPR resonance is primarily affected by the real part of $k_{sp}^{(0)}$, whereas the imaginary part relates to the damping of the propagation of the surface wave. The real part of $\Delta k_{sp}^{(1)}$ causes a displacement of the resonance position compared to $k_{sp}^{(0)}$ and $\Delta k_{sp}^{(0)}$ has an imaginary part, which causes an additional radiation damping.

The wave vector of the p-polarized incident light that is parallel to the metal surface is expressed as

$$k_x = \left(\frac{2\pi}{\lambda}\right) n_p(\lambda) \sin\,\theta, \tag{2}$$

where n_p is the refractive index of the prism, and θ is the incidence angle onto the prism. SPR takes place when the wave vector of surface plasmons matches the component of the p-polarized incident-light wave vector, which is parallel to the metal/dielectric interface ($k_{sp} = k_x$). A surface plasmon excitation is observed as a characteristic dip in the reflected light intensity spectrum.

We have calculated the physical properties of spectral sensitivity with respect to changes of resonance wavelength for the refractive index of the bulk-sensed

medium. The spectral sensitivity (S_n) under air is calculated according to a previous report (Homola 1997) and is expressed as

$$S_n = \frac{n_p \varepsilon_{mr}}{\frac{n_p}{\lambda} n_d^3 \left(\frac{1-\varepsilon_{mr}}{\varepsilon_{mr}}\right) + \frac{dn_p}{d\lambda} n_d \left(n_d^2 + \varepsilon_{mr}\right)}. \quad (3)$$

As shown in Fig. 2a, the sensitivity under air monotonically increased with respect to the wavelength. From numerical simulation, it was found that for the analysis of biomolecular interactions higher sensitivity could be obtained in the spectral SPR biosensors operated at the longer wavelength range. Even though sensitivity included the parameter of the refractive index of the prism, there was no difference of sensitivity (below 1%) between a BK-7 prism and a fused silica prism. The wavelength significantly influenced the sensitivity of the spectral SPR biosensors in Eq. 3.

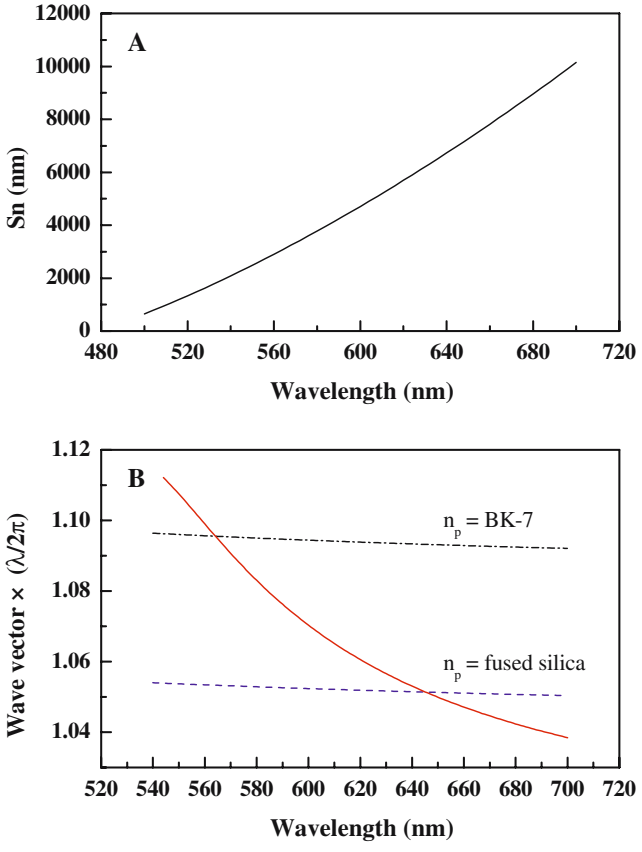

Fig. 2 Theoretical sensitivity S_n and dispersion relations. **a** Sensitivity S_n was calculated as a function of wavelength for the refractive index (n_d) of air. The dielectric constants of gold and BK-7 prism (from Schröder 1981) were used for the calculation of sensitivity. **b** The wave vector of the surface plasmon is displayed by a *solid line*. The incident-light wave vector parallel to the interface is displayed by a *dash-dotted line* for the BK-7 prism and by a *dashed line* for the fused silica prism with an incidence angle of 46.2°. The resonance wavelengths were calculated at the intersection point between the *solid line* and the *dash-dotted line* (BK-7 prism), or the *dashed line* (fused silica prism) from the graph

The theoretical dispersion relations were calculated by using a previous report for a prism/Au film/air three-phase system (Raether 1988). The resonance angle of 46.2° was determined by considering the signal acquisition, because it was possible to obtain simultaneously the long and short ranges of resonance wavelengths with one spectrometer. According to the calculated dispersion relations, resonance wavelengths of SPR biosensors with a BK-7 prism and a fused silica prism were calculated to be 564 and 645 nm, respectively, for the same incidence angle of 46.2°. As shown in Fig. 2a, the theoretical S_n showed a monotonic increase with increasing wavelength, so that it was found that the sensitivity of spectral SPR biosensors with a fused silica prism was higher than that with a BK-7 prism for the same incidence angle. It is well known that the wave vector k_x of incidence light increases with increasing refractive index of the prism, whereas the wave vector k_{sp} of the surface plasmon decreases with increasing wavelength from the dispersion relations (Akimoto et al. 1997). According to the resonance condition, the wave vector k_x should match the wave vector k_{sp} of the surface plasmon, and thus the surface plasmon's wave vector k_{sp} with longer wavelength is excited by prisms with a lower refractive index for the same incidence angle. The sensitivity S_n was calculated from Eq. 3 and the theoretical sensitivity at the resonance wavelength of 645 nm was approximately two times higher than that at the resonance wavelength of 564 nm. Consequently, this theoretical result shows that the sensitivity enhancement can be achieved not by spectral SPR biosensors with a BK-7 prism, but by spectral SPR biosensors with a fused silica prism for the same incidence angle in the analysis of protein arrays.

Results and discussion

Characterization of a gold surface and a mixed thiol surface by AFM

Gold surfaces and linker layers made of mixed thiol on gold surfaces to immobilize biomolecules without denaturation were very important factors for the analysis of protein arrays, so that the surfaces of gold and mixed thiol were investigated by AFM. The surface roughness of the metal has an influence on the optical properties of the metal surface, and also the half-width of the SPR spectrum increases with increasing roughness of the metal surface (Braundmeier and Arakawa 1974; Orlowski et al. 1979), which also affects accuracy for determining resonance wavelength near the absorption peak of the SPR spectrum.

An AFM image in the tapping mode showed that aggregated small gold particles were uniformly distributed on a gold surface, which was good enough to analyze biomolecular interactions because the gold surface roughness was below 10 Å. A surface of a mixed thiol layer was also similar to that of gold, and thus it

was difficult to distinguish a difference between them by AFM images in the tapping mode (data not shown). We investigated the surface of gold and the mixed thiol layer by the contact-mode AFM. An AFM image of the mixed thiol surface on a gold substrate was shown in Fig. 3b, compared to that of a bare gold surface (Fig. 3a). It was observed that the mixed thiol layer to immobilize biomolecules was formed on a gold substrate because a square hole (1×1 μm^2) stretched by the contact mode was not shown in the gold AFM image, but was only shown in the mixed thiol AFM image as shown in Fig. 3b. It has been reported that the molecules near these defect sites appeared to diffuse laterally and subsequently repaired the initial self-assembled monolayer (Krämer et al. 2003). However, there were two significant peaks at the edge of the square hole according to the section analysis of an AFM image in Fig. 3b. The two peaks at the edge of the square hole can be explained by the piled mixed thiol compounds due to the scratch by AFM.

From the above results, it was concluded that a linker layer made of MUA and mercaptohexanol was formed on the gold substrates and the gold surface was good enough to analyze biomolecular interactions on protein arrays.

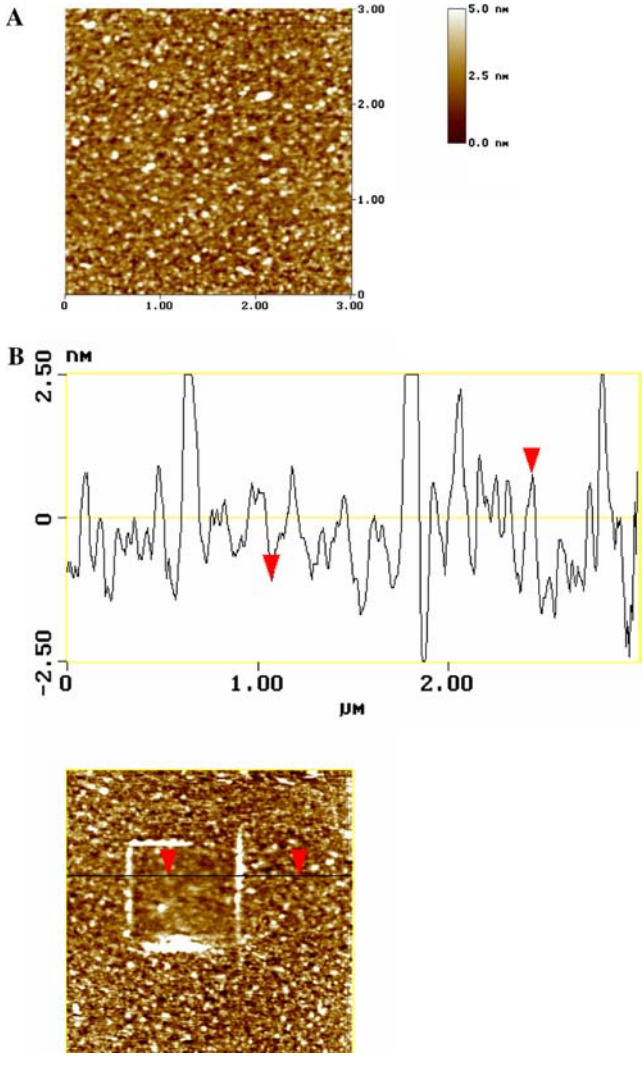

Fig. 3 Characterization of the gold and the mixed thiol surfaces. AFM imaging was performed under air by the contact mode of a Nanoscope IIIa as explained in the section under "Materials and methods". Surface topology of (**a**) a gold surface and (**b**) a mixed thiol layer. An *upper figure* of (**b**) shows the section analysis of a square hole in the mixed thiol layer

Sensitivity of spectral SPR biosensors with a BK-7 prism

In order to verify the theoretical result that sensitivity of spectral SPR biosensors was affected by the refractive index of prisms at the same incidence angle, we performed experiments on sensitivity enhancement by using specific interactions of GST–PBD on protein arrays. Specific interactions of antigens with their antibodies to form stable complexes are a basic principle of immunoassay. The analysis of antigen–antibody interactions has important applications in clinical and medical diagnostics, environmental analysis, and the food industry (Luppa et al. 2001).

As shown in Fig. 4a, we obtained serial SPR spectra after successive incubation of anti-GST and GST–PBD on the arrays modified with mixed thiol. It is well known that GSTs are major phase II detoxification enzymes found mainly in the cytosol and have peroxidase and isomerase activity. They can inhibit the Jun N-terminal kinase (thus protecting cells against H_2O_2-induced cell death) and are able to bind noncatalytically a wide range of endogenous and exogenous ligands (Sheehan et al. 2001). We obtained an SPR spectrum of a gold surface with 562 nm resonance wavelength. The resonance wavelength was calculated by the fourth-order polynomial curve fitting technique from an average SPR spectrum which was obtained by three measurements. There was a small shift of SPR spectrum caused by modification with mixed thiol on a gold surface, which could be explained by the low molecular weight and short length (below 1 nm) of mixed thiol. Resonance wavelength of the mixed thiol layer increased by 4.6 nm from that of a gold surface was an evidence of the formation of a linker layer to immobilize biomolecules, which was consistent with the earlier AFM analysis. The immobilization of GST–PBD on the mixed thiol surface was analyzed by a large shift of the SPR spectrum from the SPR spectrum of mixed thiol, and the interactions of anti-GST and GST–PBD were also clearly analyzed by shift of the SPR spectrum in Fig. 4a. The shift of resonance wavelength due to the biomolecular interactions could be explained by the increase of refractive index and thickness increment on the surface of gold (Yuk et al. 2003; Swalen et al. 1980). For the analysis of the sensitivity of spectral SPR biosensors with respect to the refractive index of prisms, we calculated the net shifts of resonance wavelength by subtracting the resonance wavelength obtained on a gold surface from that obtained after

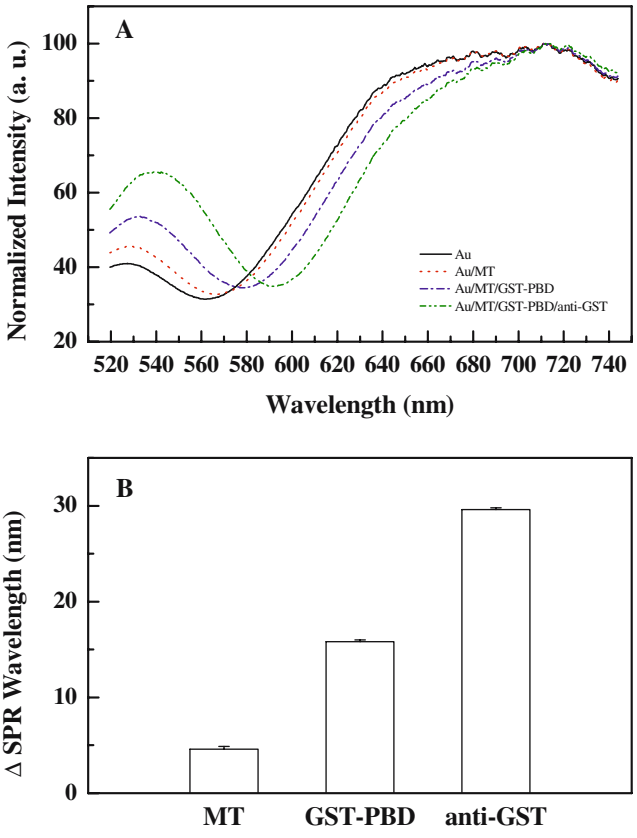

Fig. 4 SPR spectra of a spectral SPR biosensor with a BK-7 prism and net shifts of the resonance wavelength. **a** SPR spectra obtained by the spectral SPR biosensor from a gold array successively modified with a mixed thiol, GST–PBD, and anti-GST; then, the protein arrays of each incubation step were analyzed by the SPR biosensor. **b** Net shifts of the resonance wavelength were calculated by subtracting the resonance wavelength of the gold surface from that of every incubation step

successive incubation on the gold surface. As shown in Fig. 4b, the net shift of resonance wavelength increased at every incubation step, which represented the relative amount of proteins bound on the gold surfaces of protein arrays.

Sensitivity of spectral SPR biosensors with a fused silica prism

To compare the sensitivity between an SPR biosensor with a BK-7 prism and the one with a fused silica prism, we investigated shifts of resonance wavelength with the same protein arrays used in the earlier experiments by using an SPR biosensor with a fused silica prism. As shown in Fig. 5a, the resonance wavelength of a bare gold surface was 645.6 nm, which was higher by approximately 84 nm than that measured by the SPR biosensor with a BK-7 prism, and the results were consistent with the theoretical results. The wave vector of k_x decreased with decreasing refractive index of the prism for the same incidence angle in Eq. 3, so that the resonance wavelength increased to fulfill the resonance matching condition as shown in Fig. 2b. Resonance wavelengths increased on successive modification of gold array surfaces with mixed thiol, GST–PBT, and anti-GST. The results were consistent with earlier experimental results for a BK-7 prism; however, ranges and shifts of the resonance wavelength were higher than those obtained with a BK-7 prism. Sensitivity of the spectral SPR biosensor with a BK-7 prism and a fused silica prism was compared by analyzing net shifts of the resonance wavelength obtained from the same protein array. As shown in Fig. 5b, at every incubation step the net shifts of the resonance wavelength were higher with the SPR biosensor with a fused silica prism than those with the SPR biosensor with a BK-7 prism. After incubation of GST–PBD on the mixed thiol surface, net shifts of the resonance wavelength of the SPR biosensor with a fused silica prism were 1.6 times higher than those

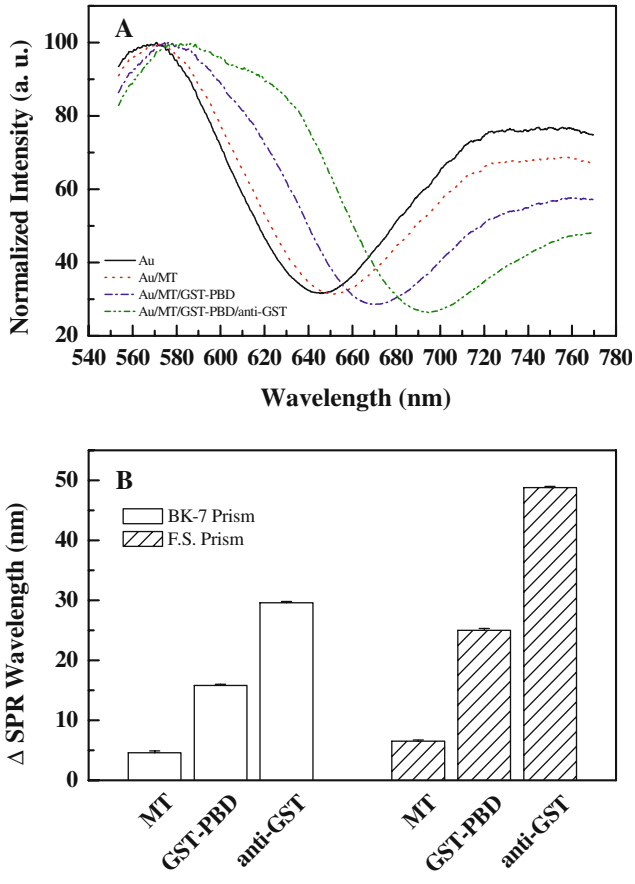

Fig. 5 SPR spectra of a spectral SPR biosensor with a fused silica prism and net shifts of resonance wavelength obtained from spectral SPR biosensors with two different prisms. **a** Gold surfaces were successively modified by mixed thiol, GST–PBD, and anti-GST, and then the protein arrays of each incubation step were analyzed by the spectral SPR biosensor. **b** Net shifts of resonance wavelength were calculated by subtracting the resonance wavelength of a gold surface from that of each modified surface. In order to compare the sensitivity of the SPR biosensors with two different prisms, the net shifts of resonance wavelength of Fig. 4b were added in (**b**)

of the SPR biosensor with a BK-7 prism. After final interactions of anti-GST and GST–PBD on protein arrays, the SPR biosensor with a fused silica prism also showed 1.6 times higher net shifts of resonance wavelength than the SPR biosensor with a BK-7 prism at the same incidence angle of 46.2°. The results show that the spectral SPR biosensor with a fused silica prism is more sensitive than that with a BK-7 prism at the same incidence angle, and spectral SPR biosensors can easily achieve sensitivity enhancement by reducing the refractive index of the prism without any additional process such as colloidal Au or certain proteins for the analysis of biomolecular interactions on protein arrays.

There were large intensity shifts due to the protein interactions at the wavelength of 540 nm in Fig. 4a and 630 nm in Fig. 5a, compared with the resonance wavelength shifts. However, the intensity of the SPR spectra was not absolute, but relative value normalized with the maximal intensity of SPR signals. We used normalized intensity-SPR spectrum for the analysis of biomolecular interactions because there was intensity fluctuation of the light. In addition, array detectors of spectrometers might be affected by sensitivity and offset between pixels. Thus, resonance wavelengths can provide more accurate meanings than normalized intensity.

It was useful to compare characteristics of spectral SPR sensors with those of monochromatic angle-scanning SPR sensors for the analysis of biomolecular interactions. The sensitivity of monochromatic angle-scanning SPR sensors on changes of refractive index increases with the decrease of operation wavelength. However, the sensitivity of spectral SPR sensors increases with the increase of the wavelength (Homola et al. 1999). In addition, the sensitivity of both spectral SPR sensors and monochromatic angle-scanning SPR sensors based on ATR prism couplers is higher than that of the SPR sensors with grating couplers so that SPR sensors using ATR prism couplers are advantages in the analysis of low concentration biomolecular interactions.

It is well known that SPR biosensors detect the changes of refractive index within the penetration depth of the evanescent field wave defined as the distance at which its maximum intensity has decayed to $1/e$ of that at the metal/dielectric interface. Changes of SPR response are related to the evanescent field intensity at the metal/dielectric interface. It can be postulated that the sensitivity was dependent on the penetration depth because the evanescent field intensity was correlated with the penetration depth (Liedberg et al. 1993). To confirm this postulate, the penetration depth at the metal/dielectric interface was calculated according to a previous report (Liedberg et al. 1993):

$$\delta = \frac{\lambda}{2\pi}\left[\frac{\varepsilon_{mr}(\lambda)+\varepsilon_a}{-\varepsilon_a^2}\right]^{1/2}, \quad (4)$$

where λ is the resonance wavelength of a gold surface, and ε_a is the dielectric constant of air. In this theoretical calculation, the effect of the thickness of proteins on the metal surface was neglected because the thickness of proteins was very thin, typically ≤ 10 nm (Nygren et al. 1987; Lee et al. 2002). It was calculated that the penetration depth of the spectral SPR biosensor with a fused silica prism was 1.7 times higher than that of the spectral SPR biosensor with a BK-7 prism. This was interpreted by increment of the penetration depth causing the sensitivity enhancement of the SPR biosensor with a fused silica prism at the same incidence angle. From the above results, it is suggested that the sensitivity enhancement for the analysis of biomolecular interactions on protein arrays is easily achieved by reducing the refractive index of the sensing prism of spectral SPR biosensors to be operated at long wavelength ranges.

Conclusions

We have demonstrated a novel method to enhance the sensitivity in the analysis of protein arrays by reducing the refractive index of the sensing prism of spectral SPR biosensors. The formation of a self-assembled monolayer with mixed thiol was confirmed by AFM imaging and SPR spectra. Sensitivity of spectral SPR biosensors with a fused silica prism was 1.6 times higher than that with a BK-7 prism in the analysis of antigen–antibody interactions of GST–PBD. Sensitivity enhancement was explained by the increment of the penetration depth on the metal/dielectric surface for the spectral SPR biosensors. Therefore, it is suggested that the sensitivity enhancement is achieved by reducing the refractive index of the sensing prism of spectral SPR biosensors to be operated at long wavelength ranges in the analysis of protein arrays.

Acknowledgments This work was supported in part by grant from the Ministry of Commerce, Industry and Energy, Republic of Korea.

References

Akimoto T, Sasaki S, Ikebukuro K, Karube I (2000) Effect of incident angle of light on sensitivity and detection limit for layers of antibody with surface plasmon resonance spectroscopy. Biosens Bioelectron 15:355–362

Akimoto T, Sasaki S, Ikebukuro K, Karube I (1997) Refractive-index and thickness sensitivity in surface plasmon resonance spectroscopy. Appl Opt 19:4058–4064

Braundmeier AJ, Arakawa ET (1974) Effect of surface roughness on surface plasmon absorption. J Phys Chem Solid 35:517–520

Haab BB, Dunham MJ, Brown PO (2001) Protein microarrays for highly parallel detection and quantitation of specific proteins and antibodies in complex solutions. Genome Biol 2: Research 0004.1–0004.13

Hanning A, Roeraade J, Delrow JJ, Jorgenson RC (1999) Enhanced sensitivity of wavelength modulated surface plasmon resonance devices using dispersion from a dye solution. Sens Actuators B 54:25–36

Homola J (1997) On the sensitivity of surface plasmon resonance sensors with spectral interrogation. Sens Actuators B 41:207–211

Homola J, Koudela I, Yee SS (1999) Surface plasmon resonance sensors based on diffraction gratings and prism couplers: sensitivity comparison. Sens Actuators B 54:16–24

Knobloch H, Szada-Borryszkowski GV, Woigk S, Helms A, Brehmer L (1996) Dispersive surface plasmon microscopy for the characterization of ultrathin organic films. Appl Phys Lett 69:2336–2337

Kodadek T (2001) Protein microarrays: prospects and problems. Chem Biol 8:105–115

Krämer S, Fuierer RR, Gorman CB (2003) Scanning probe lithography using self-assembled monolayers. Chem Rev 103:4367–4418

Kubitschko S, Spinke J, Bruckner T, Pohl S, Oranth N (1997) Sensitivity enhancement of optical immunosensors with nanoparticles. Anal Biochem 253:112–122

Lee KB, Park SJ, Mirkin CA, Smith JC, Mrksich M (2002) Protein nanoarrays generated by dip-pen nanolithography. Science 295:1702–1705

Leem SH, Shin I, Kweon SM, Kim SI, Kim JH, Ha KS (1997) Phospholipase D is not involved in RhoA-mediated activation of stress fiber formation. J Biochem Mol Biol 30:337–341

Li PY, Lin B, Gerstenmaier J, Cunningham BT (2004) A new method for label-free imaging of biomolecular interactions. Sens Actuators B 99:6–13

Liedberg B, Lundström I, Stenberg E (1993) Principles of biosensing with an extended coupling matrix and surface plasmon resonance. Sens Actuators B 11:63–72

Liedberg B, Nylander C, Lundström I (1983) Surface plasmon resonance for gas detection and biosensing. Sens Actuators 4:299–304

Luppa PB, Sokoll LJ, Chan DW (2001) Immunosensors-principles and applications to clinical chemistry. Clin Chim Acta 314:1–26

Lyon LA, Musick MD, Natan MJ (1998) Colloidal Au-enhanced surface plasmon resonance immunosensing. Anal Chem 70:5177–5183

Nygren H, Werthen M, Stenberg M (1987) Kinetics of antibody binding to solid-phase-immobilised antigen effect of diffusion rate limitation and steric interaction. J Immunol Methods 101:63–71

Okumura A, Sato Y, Kyo M, Kawaguchi H (2005) Point mutation detection with the sandwich method employing hydrogel nanospheres by the surface plasmon resonance imaging technique. Anal Biochem 339:328–337

Orlowski R, Urner P, Hornauer DL (1979) Influence of various underlayers on the surface roughness of evaporated silver films. Surf Sci 82:69–78

Pockrand I (1978) Surface plasma oscillations at silver surfaces with thin transparent and absorbing coatings. Surf Sci 72:577–588

Raether H (1988) Surface plasmons on smooth and rough surfaces and on gratings. Springer tracts in modern physics, vol 111. Springer, Berlin Heidelberg New York, Chap. 1

Schröder U (1981) Der einfluss dünner metallischer deckschichten auf die dispersion von oberflächenplasmaschwingungen in gold-silber-schichtsystemen. Surf Sci 102:118–130; Optics Guide, Melles Griot, 1999, pp 4.13

Sheehan D, Meade G, Foley VM, Dowd CA (2001) Structure, function and evolution of glutathione transferases: implications for classification of non-mammalian members of an ancient enzyme superfamily. Biochem J 360:1–16

Swalen JD, Gordon JG, Philpott MR, Brillante A, Pockrand I, Santo R (1980) Plasmon surface polariton dispersion by direct optical observation. Am J Phys 48:669–672

Wilson DS, Nock S (2001) Functional protein microarrays. Curr Opin Chem Biol 6:81–85

Wink T, Van Zuilen SJ, Bult A, Van Bennekom WP (1998) Liposome-mediated enhancement of the sensitivity in immunoassays of proteins and peptides in surface plasmon resonance spectrometry. Anal Chem 70:827–832

Yuk JS, Ha KS (2005) Proteomic applications of SPR biosensors: analysis of protein arrays. Exp Mol Med 37:1–10

Yuk JS, Jung JW, Jung SH, Han JA, Kim YM, Ha KS (2005) Sensitivity of ex situ and in situ spectral surface plasmon resonance sensors in the analysis of protein arrays. Biosens Bioelectron 20:2189–2196

Yuk JS, Yi SJ, Lee HG, Lee HJ, Kim YM, Ha KS (2003) Characterization of surface plasmon resonance wavelength by changes of protein concentration on protein chips. Sens Actuators B 94:161–164

Zhu H, Bilgin M, Bangham R, Hall D, Casamayor A, Bertone P, Lan N, Jansen R, Bidlingmaier S, Houfek T, Mitchell T, Miller P, Dean RA, Gerstein M, Snyder M (2001) Global analysis of protein activities using proteome chips. Science 293:2101–2105

Zhu H, Snyder M (2003) Protein chip technology. Curr Opin Chem Biol 7:55–63